Regular Article

blood

HEMATOPOIESIS AND STEM CELLS

# Osteoblasts support megakaryopoiesis through production of interleukin-9

Min Xiao,[1,2,*] Yongkui Wang,[1,2,*] Chen Tao,[1] Zhenyu Wang,[2] Jun Yang,[1] Zhenguo Chen,[1] Zhipeng Zou,[1] Mangmang Li,[1] Anling Liu,[1] Chunhong Jia,[1] Bin Huang,[2] Bo Yan,[2] Pinglin Lai,[2] Changhai Ding,[1] Daozhang Cai,[2] Guozhi Xiao,[3,4] Yu Jiang,[5] and Xiaochun Bai[1,2]

[1]State Key Laboratory of Organ Failure Research, Department of Cell Biology, School of Basic Medical Sciences and [2]Academy of Orthopedics, Guangdong Province, The Third Affiliated Hospital, Southern Medical University, Guangzhou, China; [3]Department of Biology and Shenzhen Key Laboratory of Cell Microenvironment, Southern University of Science and Technology, Shenzhen, China; [4]Department of Orthopedic Surgery, Rush University Medical Center, Chicago, IL; and [5]Department of Pharmacology and Chemical Biology, University of Pittsburgh School of Medicine, Pittsburgh, PA

## Key Points

- Osteoblast-produced IL-9 supports megakaryopoiesis and platelet formation.
- IL-9 is a promising therapeutic agent for treatment of thrombocytopenia.

**Severe thrombocytopenia is a significant challenge in patients undergoing myelosuppressive chemotherapy for malignancies. Understanding the biology of platelet-producing megakaryocytes development in the bone marrow microenvironment may facilitate the development of novel therapies to stimulate platelet production and prevent thrombocytopenia. We report here that osteoblasts supported megakaryopoiesis by secreting interleukin-9 (IL-9), which stimulated IL-9 receptor (IL-9R)/Stat3 signaling in promoting megakaryopoiesis. IL-9 production in osteoblasts was negatively regulated by the mechanistic target of rapamycin complex 1 (mTORC1) signaling in a NF-κB–dependent manner. Constitutive activation of mTORC1 inhibited IL-9 production in osteoblasts and suppressed megakaryocytic cells expansion, whereas mTORC1 inactivation increased IL-9 production and enhanced megakaryocyte and platelet numbers in mice. In mouse models, we showed that IL-9 administration stimulated megakaryopoiesis, whereas neutralizing endogenous IL-9 or IL-9R depletion inhibited the process. Importantly, we found that low doses of IL-9 efficiently prevented chemotherapy-induced thrombocytopenia (CIT) and accelerated platelet recovery after CIT. These data indicate that IL-9 is an essential regulator of megakaryopoiesis and a promising therapeutic agent for treatment of thrombocytopenia such as CIT. (*Blood*. 2017;129(24):3196-3209)**

## Introduction

Circulating blood platelets are specialized cells that prevent bleeding and minimize blood vessel injury.[1] Large progenitor cells in the bone marrow (BM) called megakaryocyte (MK) are the source of platelets. Megakaryopoiesis is the process by which mature MK are derived from pluripotent hematopoietic stem cells (HSCs) in the BM microenvironment. $CD41^+CD34^+$ cells arise from HSCs and proliferate and differentiate into platelet-producing mature MK, which undergo endomitosis, granule formation, proplatelet formation, and terminal platelet formation and release.[2-4] Because platelets are essential for hemostasis, morbidity and mortality from bleeding resulting from moderate to severe thrombocytopenia is a major problem facing patients with chemotherapy-induced thrombocytopenia (CIT), immune thrombocytopenia, and hepatitis C–related thrombocytopenia.[5-7]

Although blood disorders arise primarily from defects in hematopoietic cells, contextual signals from multiple cell types in the BM microenvironment or niche are also critical for disease development.[7,8] Among these cell types, osteoblasts play an important role in controlling multiple hematopoietic lineages.[9,10] Several groups have shown the importance of osteoblastic cells to the HSC niche in the BM.[11-13] Beyond their support for HSCs, osteoblasts directly regulate erythropoiesis and the maturation and differentiation of B lymphocytes.[14,15] Osteoblasts may produce many cytokines that are critical for normal hematopoiesis.[14,16]

Megakaryocytopoiesis and platelet production also occur within the BM microenvironment in highly specialized osteoblastic and vascular niches, where gradients of chemokines, growth factors, calcium, oxygen, and adhesive interactions drive MK proliferation, maturation, and thrombopoiesis. MK may promote osteoblastic bone formation in vitro and in vivo[17-19]; however, there is no in vivo evidence that osteoblasts regulate megakaryopoiesis directly or indirectly. Furthermore, little is known about the mechanisms by which osteoblasts regulate megakaryopoiesis and platelet formation. Understanding the biology of MK niches may uncover new drug targets and facilitate the development of novel therapies to stimulate platelet production and prevent thrombocytopenia.

In this study, we show that osteoblasts produce interleukin-9 (IL-9) to promote $CD41^+Sca\text{-}1^+$ cell expansion and megakaryopoiesis via stimulation of IL-9 receptor (IL-9R)/Stat3 signaling. The mammalian

Submitted 3 November 2016; accepted 19 April 2017. Prepublished online as *Blood* First Edition paper, 27 April 2017; DOI 10.1182/blood-2016-11-749838.

*M.X. and Y.W. contributed equally to this work.

The data reported in this article have been deposited in the Gene Expression Omnibus database (accession number GSE74781).

The online version of this article contains a data supplement.

The publication costs of this article were defrayed in part by page charge payment. Therefore, and solely to indicate this fact, this article is hereby marked "advertisement" in accordance with 18 USC section 1734.

target of rapamycin complex 1 (mTORC1) signaling pathway, a major regulator of cell metabolism, growth, proliferation, and survival,[20,21] suppressed IL-9 transcription via inhibition of NF-κB in osteoblasts. Importantly, low doses of IL-9 prevented CIT and accelerated platelet recovery after CIT. These findings reveal an unexpected but essential role for osteoblasts in the modulation of megakaryopoiesis and suggest that IL-9 can serve as a therapeutic agent for the treatment of thrombocytopenia.

## Materials and methods

### General methodology

No samples, mice, or data points were excluded from the reported analyses. Samples were randomized to experimental groups in C57BL/6 and BALB/c CIT mice mode, but not in TSC1 or Raptor knockout (KO) mice. Analyses were not performed in a blinded fashion.

### Cells

RAW264.7, human umbilical vein endothelial cells (HUVECs), hFOB1.19, and TM4 were obtained from the American Type Culture Collection (Manassas, VA). Human calvarial osteoblasts were obtained from Sciencell Research Laboratories (Carlsbad, CA). RAW264.7 and HUVECs were cultured in Dulbecco's modified Eagle medium (DMEM); TM4, human calvarial osteoblasts, and hFOB1.19 cells were maintained in 1:1 DMEM and Ham's F-12 medium with 10% fetal bovine serum (FBS), 100 U/mL penicillin, and 100 μg/mL streptomycin (Gibco, Paisley, Scotland) at 37°C in 5% $CO_2$. For western blot analysis, cells were plated in 6-well plates. After 24 hours, cells were treated with 50 nM rapamycin (R0395, Sigma, St. Louis, MO) for 0.5, 1, 2, and 12 hours. Cells not treated with rapamycin were used as controls. Primary osteoblastic cells were prepared from the calvaria of newborn mice, as described previously,[22,23] and cultured and exposed to rapamycin using the same method as for TM4 cells. Lymphocytes and monocytes were isolated from the BM of 8-week-old C57BL/6 mice using lymphocyte or monocyte isolation Ficoll-Paque (GE Healthcare, Little Chalfont, UK), respectively, and cultured in RPMI 1640 medium containing 10% FBS. Endothelial cells were isolated from the BM of 8-week-old C57BL/6 mice using an endothelium isolation kit (Miltenyi, Bergisch Gladbach, Germany, 130-109-679), and cultured in endothelial cell growth medium containing 10% FBS.

### Mice

Conditional KO mice were produced by interbreeding $TSC1^{fl/fl}$ (Jax#005680) or $Raptor^{fl/fl}$ (Jax#013188) mice with Osterix (OSX)-Cre (Jax#006361) and osteocalcin (OCN)-Cre (Jax#019509) mice, respectively. All mice were purchased from The Jackson Laboratory (Bar Harbor, ME). $TSC1^{fl/fl}$ or $Raptor^{fl/fl}$ littermates were used as controls for all experiments. Mice were treated with doxycycline (0.2 mg/mL in drinking water) to repress expression of OSX-Cre recombinase before they were born. Genotyping was performed on genomic DNA obtained from tail biopsies as previously described.[15] C57BL/6 and BALB/c mice (2 months old) were purchased from the Laboratory Animal Centre of Southern Medical University. The Southern Medical University Animal Care and Use Committee approved all procedures involving the mice. All animal procedures involving animals and their care were conducted in accordance with the guidelines of Animal Use and Care of the National Institutes of Health.

### Evaluation of BM MK number

The mice were euthanized by cervical dislocation, and 1 femur and 1 tibia from each mouse were used for evaluation of MK number in the BM. BM samples were smeared on the slides and stained with Wright and Giemsa dyes. The number of MK was counted under the microscope based on cell size and their previously described features.[24]

### Flow cytometry analysis

Cells were stained by standard protocols with the following antibodies (eBioscience, San Diego, CA, unless otherwise noted). BM cells were isolated as described previously,[25] and cells were incubated with antibodies. For cell lineages analysis, cells were stained with Ter119 (catalog no. 11-5921), CD11b (catalog no. 53-0112), Gr-1 (catalog no. 12-5931), CD41 (catalog no. 17-0411), and Sca-1 (catalog no. 11-5981), respectively; for MK proliferation or mTORC1 activation analysis, cells were stained with 5-ethynyl-2′-deoxyuridine (Edu; Invitrogen, Carlsbad, CA) or phospho-S6 (catalog no. 12-9007-42), Sca-1, and CD41; for MK maturation status or mTORC1 activation analysis, cells were stained for CD41, CD42d (catalog no. 12-0421) or CD41, CD42d, and phospho-S6; for IL-9R analysis, cells were stained for CD41, Ter119, CD11b, CD42d, and IL-9Rs (310404; Biolegend, San Diego, CA), respectively; for integrin α2β1 level in $CD41^{+}Sca\text{-}1^{+}$ cells analysis, cells were stained with integrin α2β1 (561067; BD Biosciences, San Diego, CA), CD41, and Sca-1; and for integrin α2β1 level in $CD41^{+}CD42d^{+}$ cell analysis, cells were stained with integrin α2β1, CD41, and CD42d. To examine the ploidy of murine MK, cells were incubated in cold 70% ethanol at 4°C overnight. The cell pellets were washed with phosphate-buffered saline (PBS) and resuspended in solution containing propidium iodide (50 μg/mL) and 100 μg/mL RNAse A (Sigma); after incubation at 37°C in the dark for 1 hour, the cells were sorted and analyzed on a FACScan flow cytometer (Becton Dickinson, San Jose, CA).

### In situ hybridization

Femur and tibia tissue was dissected from the mice and fixed with 4% paraformaldehyde in PBS at 4°C for 24 hours, followed by decalcification in 15% EDTA (pH 7.4) at 4°C for 14 days. The tissue was embedded in paraffin, and 3-μm sagittal sections were cut and permeabilized with 1% Triton X-100 in PBS for 30 minutes. Cells were then washed in 2× saline-sodium citrate (SSC) with 50% formamide for 5 minutes at room temperature. Hybridization was carried out overnight at 38.5°C in hybridization buffer consisting of 10% dextran sulfate, 2 mM vanadyl ribonucleoside complex, 0.02% bovine serum albumin, and 10 ng RNA probe in 2× SSC with 50% formamide. Cells were washed with prewarmed 2× SSC with 50% formamide at 37°C for 30 minutes, washed twice in PBS, and mounted with Vectashield mounting medium (Vector Laboratories, Burlingame, CA). The sequences of sense and antisense probes corresponding to mouse 5′ IL-9 RNA are CCAAGCTTTTGCTCTTCAGTTCTGTGCTGGG and CCCAGCACAGAACTGAAGAGCAAAAGCTTGG, respectively (Invitrogen).

### In vivo treatments

Recombinant murine IL-9 (219-19; Peprotech, Rocky Hill, NJ) was reconstituted in 1× PBS and injected intraperitoneally (IP) at a dose of 1 μg/kg per day into 3-week-old OSX-TSC1 KO and wild-type (WT) mice daily for 14 days. To block IL-9 in vivo, 40 μg purified IL-9 antibody (16-7093; eBioscience) was injected into the marrow cavity of OSX-Raptor KO mice and WT littermates by bilateral intratibial injection. Mice were euthanized after 14 days of treatments, BM was collected for MK count and flow cytometry analysis, and whole blood was collected for quantitative analysis.

### Collection of conditioned medium from osteoblast, BMSC, lymphocyte, monocyte, and endothelial cells cultures

BM stromal cells (BMSCs) were isolated as previously described.[26] Osteoblast, lymphocyte, monocyte, and endothelial cells were cultured as described previously. Conditioned medium was collected when cells reached 80% to 90% confluence.

### Coculture of mouse BM cells with conditioned medium from osteoblast, BMSC, lymphocyte, monocyte, and endothelial cells

C57BL/6 mouse total BM cells were plated in 6-well plates containing DMEM: Ham's F-12 medium with 10% FBS. Cocultures were cultured with fresh medium and osteoblast, lymphocyte, BMSC, monocyte, or endothelial cells culture-conditioned medium (1:2); or with TSC1- or Raptor-null osteoblast

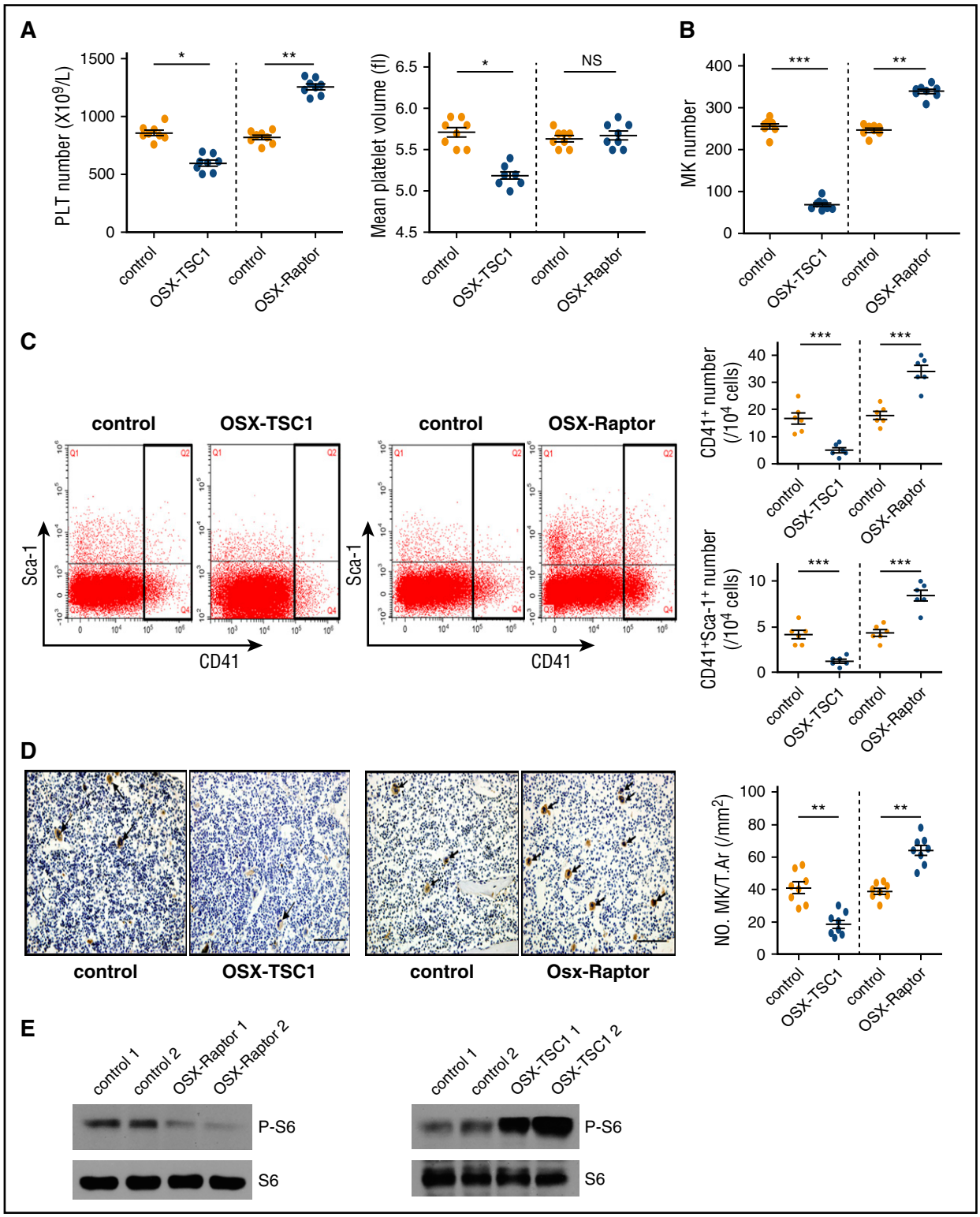


**Figure 1. mTORC1 signaling in mouse osteoblasts regulates megakaryopoiesis and platelet (PLT) formation.** (A) Platelet count and MPV in 3-week-old OSX-TSC1 and OSX-Raptor mice and control littermates (n = 8, Student unpaired *t* test). (B) BM of a femur and a tibia collected from OSX-TSC1 and OSX-Raptor mice stained with Wright and Giemsa dyes. Total numbers of MKs were counted (n = 8, Student unpaired *t* test). (C) Quantification of FACS analysis of the fraction of $CD41^+$ MK lineage cells in OSX-TSC1 and OSX-Raptor mouse BM (n = 6, Student unpaired *t* test). (D) Femur sections of OSX-TSC1 and OSX-Raptor mice stained for VWF. Cells positive for VWF were counted under a microscope. Results represent mean MK number/$mm^2$ (± standard error of the mean) for each group analyzed (40 sections from 8 mice) (n = 8, Student unpaired *t* test). Scale bar = 100 μm. (E) Western blot analysis of *p*-S6 (S235/236) expression in primary osteoblasts isolated from OSX-TSC1, OSX-Raptor, and control mice. S6 was used as a loading control. Data are representative of 3 independent experiments and are represented as mean ± standard deviation (SD). $^*P < .05$; $^{**}P < .01$; $^{***}P < .001$. NS, not significant; T.Ar, tissue area.

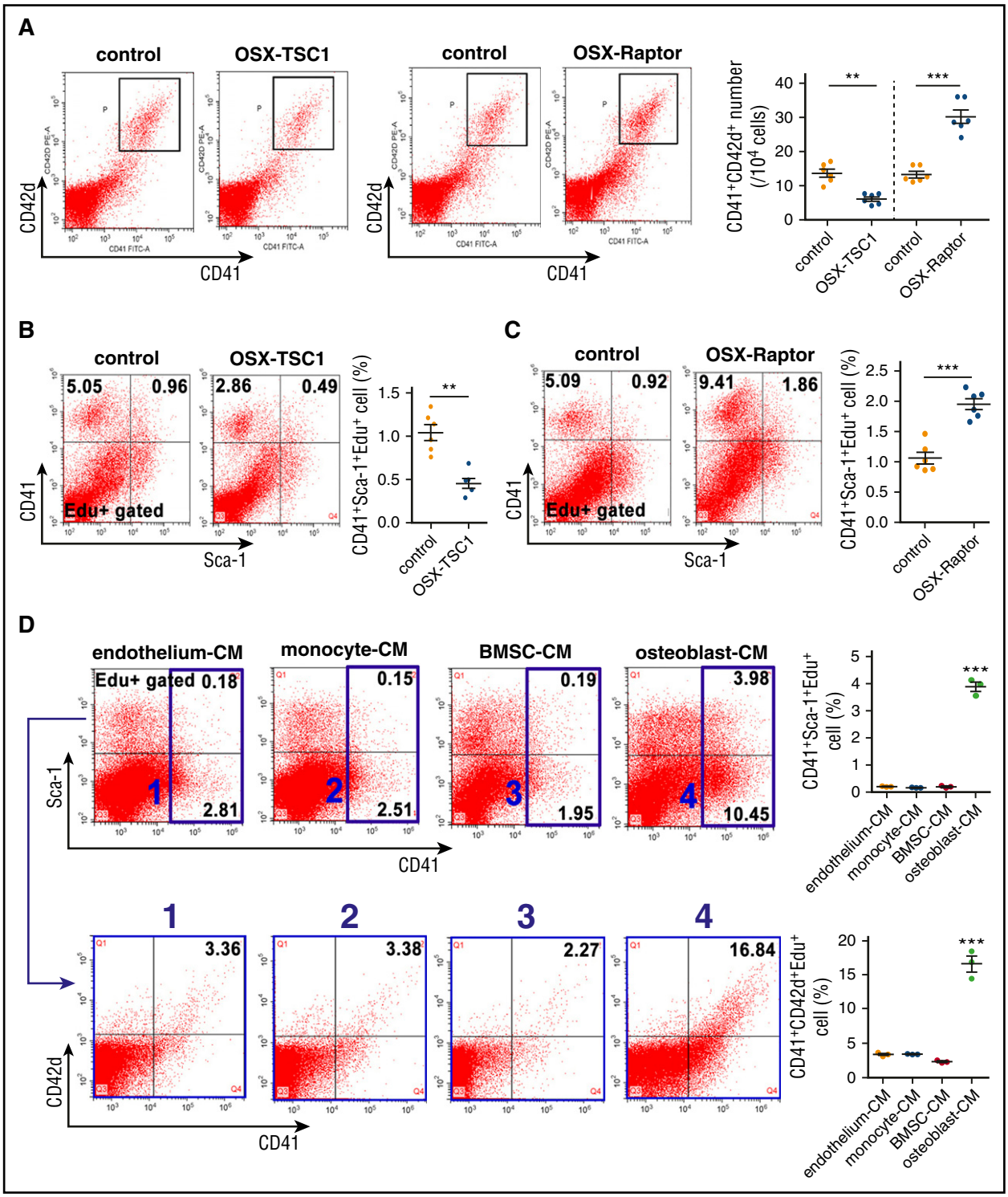


**Figure 2. Osteoblasts support MK lineage cell expansion in vitro and in vivo.** (A) Quantification of FACS analysis of the fraction of $CD41^+CD42d^+$ mature MK in BM of 3-week-old OSX-TSC1 and OSX-Raptor mice and control littermates (n = 6, Student unpaired *t* test). (B) Quantification of FACS analysis of $CD41^+Sca\text{-}1^+$ MK proliferation rates in BM of OSX-TSC1 and control littermates (n = 6, Student unpaired *t* test). (C) Quantification of FACS analysis of $CD41^+Sca\text{-}1^+$ MK proliferation rates in BM of OSX-Raptor and control mice (n = 6, Student unpaired *t* test). (D) Quantification of FACS analysis of proliferation rate of $CD41^+Sca\text{-}1^+$ and $CD41^+CD42d^+$ cells (n = 3, 1-way analysis of variance [ANOVA]). BM cells were cultured in conditioned medium (CM) from osteoblast, monocyte, BMSC, or endothelial cell culture supernatant for 4 days. The lymphoid and granulocytes were then removed from the CM-stimulated BM cells by direct lineage cell depletion kit (130-110-470; Miltenyi, Bergisch Gladbach, Germany) and the proliferation rate of $CD41^+Sca\text{-}1^+$ and $CD41^+CD42d^+$ cells was analyzed by FACS. Data are representative of 3 independent experiments and are represented as mean ± SD. $^{**}P < .01$; $^{***}P < .001$.

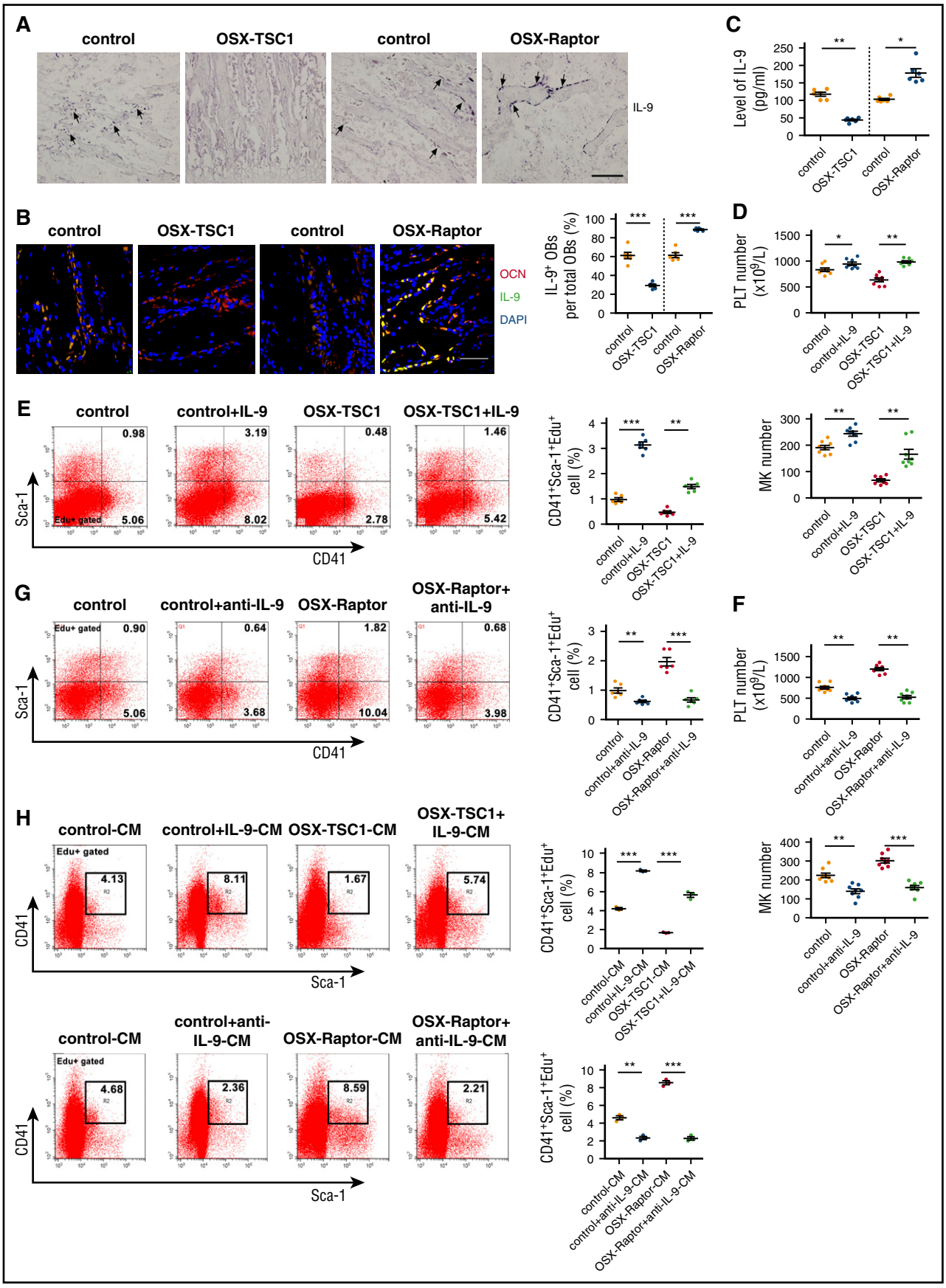


**Figure 3.**

culture-conditioned medium (1:2) with or without recombinant murine IL-9 (40 ng/mL) or purified IL-9 antibody (40 μg/mL) at days 3 and 7. Cells were harvested on day 10. All samples were analyzed by flow cytometry.

### Immunofluorescence on tissue sections

Femur and tibia tissues dissected from the mice were fixed using 4% paraformaldehyde in PBS at 4°C for 24 hours and then decalcified in 15% EDTA (pH 7.4) at 4°C for 14 days. The tissues were embedded in paraffin, and 3-μm sagittal-oriented sections were prepared for histological analyses. For immunofluorescence, we incubated primary antibodies that recognized primary antibodies against the following proteins: CD41, IL-9, osteocalcin, and *p*-STAT3 (Y705) (AP0070; Abclonal, College Park, MD) and labeled with secondary antibodies for 1 hour in the dark. After labeling, cells were incubated with 4′,6-diamidino-2-phenylindole (DAPI) for 5 minutes. The images were acquired with an Olympus 200 M microscope. We counted the numbers of positively stained cells in the whole medullary space or bone trabecula per femur or tibia in 3 sequential sections per mouse in each group with Image Pro Plus software.

### In vivo siRNA knockdown of IL-9R

Small interfering RNA (siRNA) against IL-9R (sense 5′-GUUAUGAGGA CAAGACAGATT-3′ and antisense 5′-UCUGUCUUGUCCUCAUAACTT-3′) and a control scrambled siRNA were purchased from Invitrogen. IL-9R or negative control siRNAs (10 μg/mouse) were injected into the bilateral medullary cavity of 3-week-old OSX-Raptor KO and WT mice (n = 6). Entranster in vivo transfection reagent (Engreen Biosystem, New Zealand) was used as a vehicle for siRNA delivery according to the manufacturer's recommendations. Ten days after the injection, mice were euthanized, BM was collected for MK counts and flow cytometry analysis, and whole blood was collected for quantitative analysis.

### CIT mouse model and treatment

C57BL/6 or BALB/c female mice (2 months old) were used for experiments. Carboplatin (C-2538; Sigma) was reconstituted with sterile 0.9% NaCl and injected IP at a dose of 100 mg/kg to induce thrombocytopenia. Recombinant murine IL-9 (1-7.5 μg/kg), thrombopoietin (TPO; 100 μg/kg) (315-14; Peprotech), and IL-11 (100 μg/kg) (220-11; Peprotech) were injected IP each day for varying durations starting 1 day after carboplatin injection. For platelet recovery experiments, C57BL/6 and BALB/c mice (2 months old) were injected with carboplatin (100 mg/kg) and treated 8 days later with 2.5 μg/kg IL-9 for another 8 days.

### Microarray analysis

For messenger RNA (mRNA) array assay, calvarial osteoblasts from OSX-TSC1 mice and WT mice were hybridized on an Agilent-014868 Whole Mouse Genome Microarray 4x44K G4122F (Probe Name version). Each microarray chip was hybridized to a single sample labeled with Cy3. Background subtraction and normalization were performed. mRNAs with expression levels differing by at least threefold between WT and Tsc1 null osteoblasts were selected ($P < .05$).

### Statistical analysis

All experiments were carried out in triplicate. Multiple comparisons were assessed by 1-way analysis of variance; otherwise, Student unpaired *t* test was used for statistical analysis. Results were considered significant difference at $*P < .05$; $**P < .01$; $***P < .001$.

## Results

### Osteoblasts regulate megakaryopoiesis in mice

We previously generated mice that constitutively express mTORC1 in preosteoblasts by crossing *Tsc1* (mTORC1 inhibitor)-loxP mice with OSX-Cre mice (OSX-TSC1) mice.[27] These mice exhibited immature woven bone because of excess proliferation but impaired differentiation and maturation of cells in the osteoblast lineage.[27] Interestingly, a routine blood examination revealed a significant decrease in platelet count and mean platelet volume (MPV) in OSX-TSC1 mice as compared with their littermate controls (Figure 1A), but the numbers of red blood cells and white blood cells were unaffected (see supplemental Table 1, available on the *Blood* Web site). An examination of BM cells indicated that the decrease in platelet number and MPV could result from reduced megakaryopoiesis, because quantitative analysis and fluorescent-activated cell sorting (FACS) revealed that the number of BM MK was decreased by one-third and that the number of $CD41^+$ cells were also reduced in OSX-TSC1 mice (Figure 1B-C). In contrast, no significant differences in granulocytic ($CD11b^+$), myeloid ($Gr1^+$), and erythroid ($Ter119^+$) lineages and mTORC1 activation in MKs were observed between OSX-TSC1 and control mice (supplemental Figure 1). Furthermore, analysis of femur sections also revealed fewer von Willebrand factor (VWF) (MK marker)-positive cells in OSX-TSC1 mice than in littermate controls (Figure 1D). The expression level of integrin $\alpha 2\beta 1$, a matrix receptor whose mutation or deletion in megakaryocytes results in reduced MPV in mice,[28,29] was significantly decreased in megakaryocytes of OSX-TSC1 KO mice (supplemental Figure 2). These findings suggest that mTORC1 activation in osteoblasts specifically inhibits megakaryopoiesis in mice.

We conditionally inactivated mTORC1 in osteoprogenitor cells by crossing *Raptor* (mTORC1 component)-loxP mice with OSX-Cre mice (OSX-Raptor). These mice exhibited mTORC1 inactivation in osteoblasts and slight osteoporosis, as evidenced by decreased phosphorylation of S6 (S235/236) (a marker for mTORC1 activity) (Figure 1E). Significantly, OSX-Raptor mice showed a marked increase in platelet count (Figure 1A) and the number of MK and MK lineage cells (Figure 1B-D), whereas no significant differences were observed in the development of granulocytic, myeloid, and erythroid lineages and mTORC1 activation in MKs between OSX-Raptor and control mice (supplemental Figure 1). These results demonstrate

**Figure 3. IL-9 produced by osteoblasts promotes MK lineage cell expansion and platelet formation.** (A) In situ hybridization analysis of IL-9 mRNA expression and hematoxylin and eosin staining of mouse tibia at 3 weeks. Scale bar = 100 μm. (B) IL-9 expression in the BM microenvironment. Mouse femur sections at 3 weeks were labeled with antibodies against OCN (red) and IL-9 (green). Blue, nuclear DAPI staining. Scale bar = 30 μm. (See supplemental Figure 7.) (C) IL-9 levels in BM of OSX-TSC1, OSX-Raptor, and control mice at 3 weeks (n = 6, Student unpaired *t* test). (D) Peripheral blood platelet count and MK numbers in OSX-TSC1 and control mice injected IP with recombinant murine IL-9 (1 μg/kg per day) for 14 days (n = 8, Student unpaired *t* test). (E) Quantification of FACS analysis of $CD41^+Sca\text{-}1^+$ cells proliferation ($Sca\text{-}1^+CD41^+Edu^+$) in BM of IL-9–treated mice (n = 6, Student unpaired *t* test). (F) Peripheral blood platelet count and MK numbers in OSX-Raptor and control mice bilateral intratibially injected into the marrow cavity with purified IL-9 antibody (40 μg) for 14 days (n = 8, Student unpaired *t* test). (G) Quantification of FACS analysis of proliferation rate of $CD41^+Sca\text{-}1^+$ cell proliferation ($CD41^+Sca\text{-}1^+Edu^+$) in BM of IL-9 antibody-treated mice (n = 6, Student unpaired *t* test). (H) Quantification of FACS analysis of proliferation rate of $CD41^+Sca\text{-}1^+$ cells ($CD41^+Sca\text{-}1^+Edu^+$) cultured in conditioned medium from Raptor- or TSC1-deficient osteoblast cultures supplemented with IL-9 antibody or IL-9 (n = 3, Student unpaired *t* test). Data are representative of 3 independent experiments and are represented as mean ± SD. $*P < .05$; $**P < .01$; $***P < .001$. OB, osteoblast.

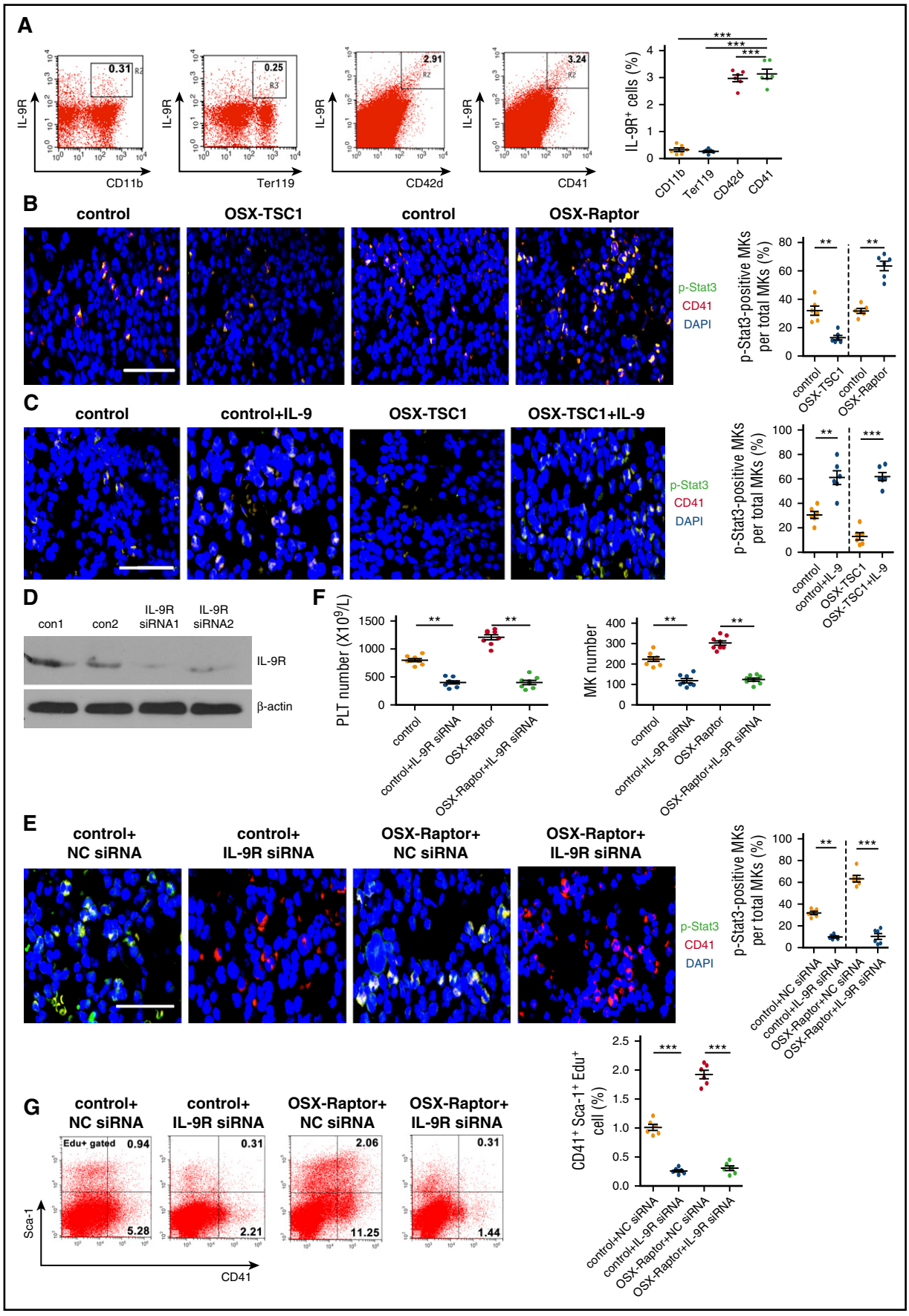


Figure 4.

that mTORC1 inhibition in osteoblasts stimulates megakaryopoiesis in mouse BM.

OSX-Cre mediates efficient Cre-recombinase activity in osteoprogenitor cells, thereby targeting the entire osteoblastic lineage.[30] To evaluate further the effect of mTORC1 inactivation in mature osteoblasts on megakaryopoiesis, we generated osteoblast-specific *Raptor* or *Tsc1* depletion mice by crossing *Raptor* or *Tsc1* loxP mice to OCN-Cre mice. Similarly, OCN-Raptor and OCN-TSC1 mice exhibited an increase and decrease, respectively, in the number of MK lineage cells and platelets without any changes in the development of other hematopoietic lineages (supplemental Figures 3 and 4). These findings indicate that mTORC1 signaling in osteoblasts controls megakaryopoiesis in mice.

### Osteoblasts support CD41$^+$Sca-1$^+$ cells expansion in vitro and in vivo

During the process of megakaryopoiesis, CD34$^+$CD41$^+$ cells proliferate and differentiate into platelet-producing mature MK (CD41$^+$CD42$^+$).[2-4] We found that the number of CD41$^+$Sca-1$^+$ cells and mature MK (CD41$^+$CD42d$^+$) decreased markedly in OSX-TSC1 mice as compared with control mice (Figures 1C and 2A). Cultured MKs with osteoblast culture supernatant produced the similar results (supplemental Figure 5). On the contrary, MK and CD41$^+$Sca-1$^+$ cells numbers were increased in OSX-Raptor mice (Figures 1C and 2A). These results suggest that osteoblastic mTORC1 may affect megakaryopoiesis by regulating the expansion of CD41$^+$Sca-1$^+$ cells. Notably, EdU staining of BM cells confirmed that the proliferation of CD41$^+$Sca-1$^+$ cells was increased in OSX-Raptor but impaired in OSX-TSC1 mice (Figure 2B-C). This evidence demonstrates that osteoblastic mTORC1 prevents CD41$^+$Sca-1$^+$ cells expansion in mice.

We next investigated whether osteoblasts regulate CD41$^+$Sca-1$^+$ cells expansion in vitro. BM cells cultured in osteoblast culture supernatant exhibited an enhancement in CD41$^+$Sca-1$^+$ and CD41$^+$CD42d$^+$ cells proliferation rate compared with cells cultured in monocyte, BMSC, or endothelial cell culture-conditioned medium (Figure 2D). Thus, osteoblasts support CD41$^+$Sca-1$^+$ cells expansion both in vivo and in vitro.

### IL-9 production by osteoblasts is essential for CD41$^+$Sca-1$^+$ cell expansion and platelet formation

The in vitro and in vivo evidence suggest that osteoblasts regulate MK expansion in a paracrine manner by modulating production of signaling molecules. To investigate which osteoblast-derived molecules were regulated by mTORC1, a global mRNA expression profile in TSC1 ablation or WT osteoblasts was developed using a microarray. Unexpectedly, levels of growth factors or cytokines known to promote megakaryopoiesis such as TPO, stem cell factor, erythropoietin, leukemia inhibitory factor, and IL-11 were unaltered in TSC1-deficient osteoblasts (supplemental Table 2). However, IL-9, a cytokine with diverse biological functions, was markedly downregulated in TSC1-null osteoblasts (supplemental Table 2). T helper cells and mast cells are major sources of IL-9 in the immune system,[31,32] but in the BM the source of IL-9 is unknown. Surprisingly, among osteoblasts, monocytes/macrophages, BMSCs, and endothelial cells, osteoblasts produced the highest level of IL-9 mRNA (supplemental Figure 6A). IL-9 could also be detected in culture of human osteoblast (supplemental Figure 7). IL-9 in situ hybridization and OCN double labeling confirmed that IL-9 was predominantly expressed by osteoblasts in the BM (Figure 3A-B; supplemental Figure 8). Furthermore, TSC1 deletion reduced, whereas Raptor depletion increased, IL-9 mRNA and protein levels in cultured osteoblasts (supplemental Figure 6B-C) and BM (Figure 3C). These results suggest that osteoblasts are the major source of IL-9 in BM and produce IL-9 in an mTORC1-dependent manner.

To investigate the role of IL-9 in megakaryopoiesis in vivo, we injected recombinant mouse IL-9 or antibody against IL-9 into mouse BM for 2 weeks. IL-9 enhanced platelet count and MPV and restored CD41$^+$Sca-1$^+$ MK proliferation in OSX-TSC1 mice (Figure 3D-E; supplemental Figure 9A) without affecting red blood cell and white blood cell numbers (supplemental Table 3). In contrast, neutralization of endogenous IL-9 using a specific antibody reduced platelet count and suppressed CD41$^+$Sca-1$^+$ MK proliferation in OSX-Raptor mice (Figure 3F-G; supplemental Figure 9B). Importantly, addition of IL-9 antibody to MK cultures abolished the stimulation of CD41$^+$Sca-1$^+$ MK proliferation (CD41$^+$Sca-1$^+$Edu$^+$) by Raptor-null osteoblast-conditioned medium (Figure 3H). Incubation of BM cultures with IL-9 restored the ability of TSC1-null osteoblast-conditioned medium to stimulate CD41$^+$Sca-1$^+$ MK proliferation (Figure 3H). Interestingly, IL-9 also increased MK ploidy and proplatelet formation (supplemental Figure 10). These results suggest that osteoblasts promote CD41$^+$Sca-1$^+$ MK expansion and megakaryopoiesis via mTORC1-dependent production of IL-9 both in vitro and in vivo.

### IL-9 promotes CD41$^+$Sca-1$^+$ cells via IL-9R/Stat3 signaling

IL-9 activates a heterodimeric receptor that consist of the IL-9R α chain (IL-9Rα) and γ chain and induces the cross-phosphorylation of JAK, leading to activation of Stat signaling and the upregulation of IL-9–induced gene transcription.[31,32] Consistent with the effects of IL-9 on hematopoietic cells, FACS analysis of mouse BM cells revealed that MK lineages (CD41$^+$ or CD42d$^+$), but not granulocytic (CD11b$^+$) or erythroid (Ter119$^+$) lineages expressed high levels of IL-9Rα (Figure 4A). Furthermore, Stat3 phosphorylation was increased in CD41$^+$ cells from OSX-Raptor mouse BM, whereas the level was lower in OSX-TSC1 mouse BM CD41$^+$ cells (Figure 4B; supplemental Figure 11). IL-9 treatment increased Stat3 phosphorylation in BM CD41$^+$ cells (Figure 4C; supplemental Figure 12). Importantly, injection of IL-9Rα siRNAs into mouse BM suppressed IL-9Rα expression and Stat3 phosphorylation in CD41$^+$ cells (Figure 4D-E; supplemental Figure 13), inhibited CD41$^+$Sca-1$^+$ MK proliferation, and reduced platelet number in WT mice (Figure 4F-G; supplemental Table 3). IL-9Rα siRNA also abolished the increase in Stat3 phosphorylation and megakaryopoiesis in OSX-Raptor

**Figure 4. IL-9 promotes MK lineage cell expansion via activation of IL-9R/Stat3 signaling.** (A) Quantification of FACS analysis of IL-9R expression in CD41$^+$ MK, CD42d$^+$ MK, CD11b$^+$ granulocytic, and Ter119$^+$ erythroid lineages in BM of 3-week-old mice (n = 6, Student unpaired *t* test). (B) Femur sections of OSX-Raptor, OSX-TSC1, or control mice at 3 weeks probed for expression of CD41 (red) and *p*-Stat3 (green). Blue, nuclear DAPI staining. Scale bar = 30 μm. (See supplemental Figure 10.) (C) Femur section of mice bilaterally injected IP with IL-9 (1 μg/kg per day) for 14 days and probed for expression of CD41 (red) and *p*-Stat3 (green). Blue, nuclear DAPI staining. Scale bar = 30 μm. (See supplemental Figure 11.) (D) OSX-Raptor and control mice at 3 weeks bilaterally intratibially injected into the marrow cavity with IL-9R or control siRNA for 10 days. The effect of specific siRNAs for IL-9R in BM cells was detected by western blot. (E) Femur section of treated mice immunolabeled for CD41 (red) and *p*-Stat3 (green). Scale bar = 20 μm. (See supplemental Figure 12.) (F) Platelet and MK counts (± standard error of the mean) of IL-9R siRNA-treat mice (n = 8, Student unpaired *t* test). (G) Quantitative analysis of proliferation rate in CD41$^+$Sca-1$^+$ cells (CD41$^+$Sca-1$^+$Edu$^+$) in BM of IL-9 siRNA-treated mice (n = 6, Student unpaired *t* test). Data are representative of 3 independent experiments and are represented as mean ± SD. $^{**}P < .01$; $^{***}P < .001$. Con, control; NC, no significance.

mice (Figure 4E-G). These findings indicate that IL-9 activates IL-9R/Stat3 signaling in CD41$^+$Sca-1$^+$ MK to promote their expansion and megakaryopoiesis.

### mTORC1 inhibits NF-κB signaling to suppress IL-9 transcription in osteoblasts

We next explored the mechanism by which mTORC1 inhibits IL-9 expression in osteoblasts. Several transcription factors were reported to regulate the *Il9* gene transcription and were required for the development of IL-9–secreting cells.[33] Among these factors, NF-κB is activated by mTORC1 in cancer cells[34] and is essential for IL-9 transcription by binding to *Il9* gene promoter in mast cells.[35] Unexpectedly, NF-κB activity was strongly inhibited in TSC1-deficient osteoblasts with constitutive mTORC1 activation, as manifested by the markedly reduced phosphorylation and nuclear localization of p65 NF-κB (S653) (Figure 5A-B). Electrophoretic mobility shift assay (EMSA) confirmed the reduced binding of NF-κB to the *Il9* promoter in TSC1-deficient osteoblasts (Figure 5C). On the contrary, NF-κB was activated in Raptor-deficient osteoblasts in which mTORC1 was inhibited (Figure 5D-F). The change in NF-κB activity was associated with IL-9 expression in osteoblasts. Importantly, inhibition of NF-κB abrogated the enhanced IL-9 expression in Raptor-deficient osteoblasts (Figure 5G). Rapamycin treatment stimulated NF-κB activity and IL-9 expression in osteoblasts (Figure 5H-I). The stimulatory effects of the drug on IL-9 expression were blocked by inhibition of NF-κB (Figure 5I). These findings demonstrate that mTORC1 represses IL-9 expression through inhibition of NF-κB signaling.

Several studies have reported that mTORC1 activates NF-κB downstream of Akt and upstream of inhibitor of NF-κB kinase (IKK) in tumor cells.[34,36] To confirm the negative regulation of NF-κB by mTORC1, we tested a variety of cells including osteoblasts, TSC2-deficient mouse embryonic fibroblasts (TSC2$^{-/-}$ MEFs), monocytes (Raw264.7), Sertoli cells (TM4), and HUVECs. Hyperactivation of mTORC1 in TSC1-null osteoblasts or TSC$^{-/-}$ MEFs strongly reduced phosphorylation of IKK-α/β (S180/181) and p65 NF-κB, while blocking mTORC1 by rapamycin-enhanced phosphorylation of IKK-α/β and p65 NF-κB in all examined cells (supplemental Figure 14A-B). These observations support the negative regulation of IKK/NF-κB signaling by mTORC1. Because Akt is critical for activation of IKK/NF-κB signaling in many cells, we surmised that activated mTORC1 suppresses IKK/NF-κB signaling by inhibiting Akt activity via several negative feedback loops.[21] Indeed, we found that phosphorylation of Akt at S473 and T308 was abrogated in mTORC1-hyperactivated osteoblasts (TSC1 null) and enhanced in mTORC1-inactivated osteoblasts (Raptor-null or rapamycin treatment) (supplemental Figure 14C). In addition, pharmacological inhibition of PI-3K/Akt repressed IL-9 expression in both WT and Raptor-null osteoblasts (Figure 5I). These results suggest that mTORC1 may repress IKK/NF-κB through negative feedback inhibition of Akt.

### Low doses of IL-9 prevent CIT and accelerate platelet recovery after thrombocytopenia

CIT is a common problem in cancer patients. Aside from bleeding risk, thrombocytopenia limits chemotherapy dose and frequency.[37] Based on the thrombopoietic effects of IL-9 described previously, we assessed its potential application in the treatment of CIT in mice. Severe thrombocytopenia was induced in C57BL/6 and BALB/c mice (2 months old) by administering a high dose of carboplatin (100 mg/kg) for 8 days (Figure 6A-B; supplemental Table 4). Interestingly, in addition to thrombocytopenia, carboplatin reduced the number of osteoblasts and the IL-9 level in BM (supplemental Figure 15); however, the drug-induced thrombocytopenia was completely blocked by treatment with low doses of recombinant mouse IL-9. IL-9 was more effective than TPO and IL-11, 2 cytokines commonly used to treat CIT patients, because the dose required to completely block thrombocytopenia was much lower (100 μg/kg per day for TPO and IL-11) (Figure 6). Furthermore, a low dose of IL-9 accelerated the recovery of megakaryopoiesis and platelet count resulting from high-dose CIT in mice (Figure 7A-B). These findings demonstrate that IL-9 can effectively prevent CIT and accelerate platelet recovery after thrombocytopenia, suggesting that IL-9 is a promising candidate for CIT treatment.

## Discussion

Postnatal hematopoiesis occurs almost entirely in the BM close to or at endosteal surfaces, and many studies have investigated the molecular and cellular interactions between hematopoietic cells and osteoblast lineage cells.[8,10,13] MK directly stimulates osteoblast proliferation and differentiation.[18,19] However, there is no in vivo evidence for direct or indirect regulation of megakaryopoiesis by osteoblasts. In addition to previously known cytokines that support hematopoiesis, we found that osteoblasts produced a high level of IL-9, implying a specific function for osteoblast-secreted IL-9 in BM. Our in vivo and in vitro evidence demonstrate the essential role of osteoblasts in supporting CD41$^+$Sca-1$^+$ MK expansion, megakaryopoiesis, and platelet formation via IL-9 production, underscoring the important contribution of osteoblasts to the BM microenvironment and megakaryopoiesis (Figure 7C). Cells of osteoblast lineage are a heterogeneous population consisting of BMSCs and osteoblasts at different stages of differentiation. Several lines of evidence suggest that mature osteoblasts are important for CD41$^+$Sca-1$^+$ MK expansion: first, loss of TSC1 or Raptor in osteoblasts (OCN-Cre) had similar effects on megakaryopoiesis as osteoprogenitor- and osteoblast (OSX-Cre)-specific deletion; second, BMSCs produced less IL-9 than mature osteoblasts; and, finally, mTORC1 activity declined during the differentiation of osteoblasts from BMSCs[27] and inhibited megakaryopoiesis.

Although many biological functions have been attributed to IL-9, it remains an understudied cytokine. Beyond the major description as a T-cell or mast-cell growth factor, IL-9 may affect other immune cells, as well as resident tissue cells that contribute to the development of inflammation.[32] The diverse functions of IL-9 are mediated by IL-9Rs, which consist of the cytokine-specific α chain and the γ chain shared by other cytokine receptors, such as those for IL-2, IL-4, and IL-7. Ligand binding to the cognate receptor activates JAK/Stat signaling in target cells.[32,33] Although IL-9 originally was identified as a hematopoietic cell regulatory factor,[33] it has been reported to potentiate MK expansion in culture in the presence of TPO and/or stem cell factor.[38] However, its role in megakaryopoiesis in vivo is unknown. Interestingly, a recent study found that IL-9R expression is upregulated by eightfold during in vitro MK development, implying that it has a role in megakaryopoiesis.[37] Our finding that neutralizing IL-9 or knocking down IL-9R prevented megakaryopoiesis suggests an important role for IL-9/IL-9R in this process.

mTOR signaling integrates diverse signals to control cell growth, proliferation, differentiation, and metabolism.[21] The present study showed that mTORC1 activation in osteoblasts prevented CD41$^+$Sca-1$^+$ MK proliferation via downregulation of NF-κB–dependent IL-9 production, implying that low osteoblastic mTORC1 activity is important for megakaryopoiesis. Osteoblasts modulate the physiological

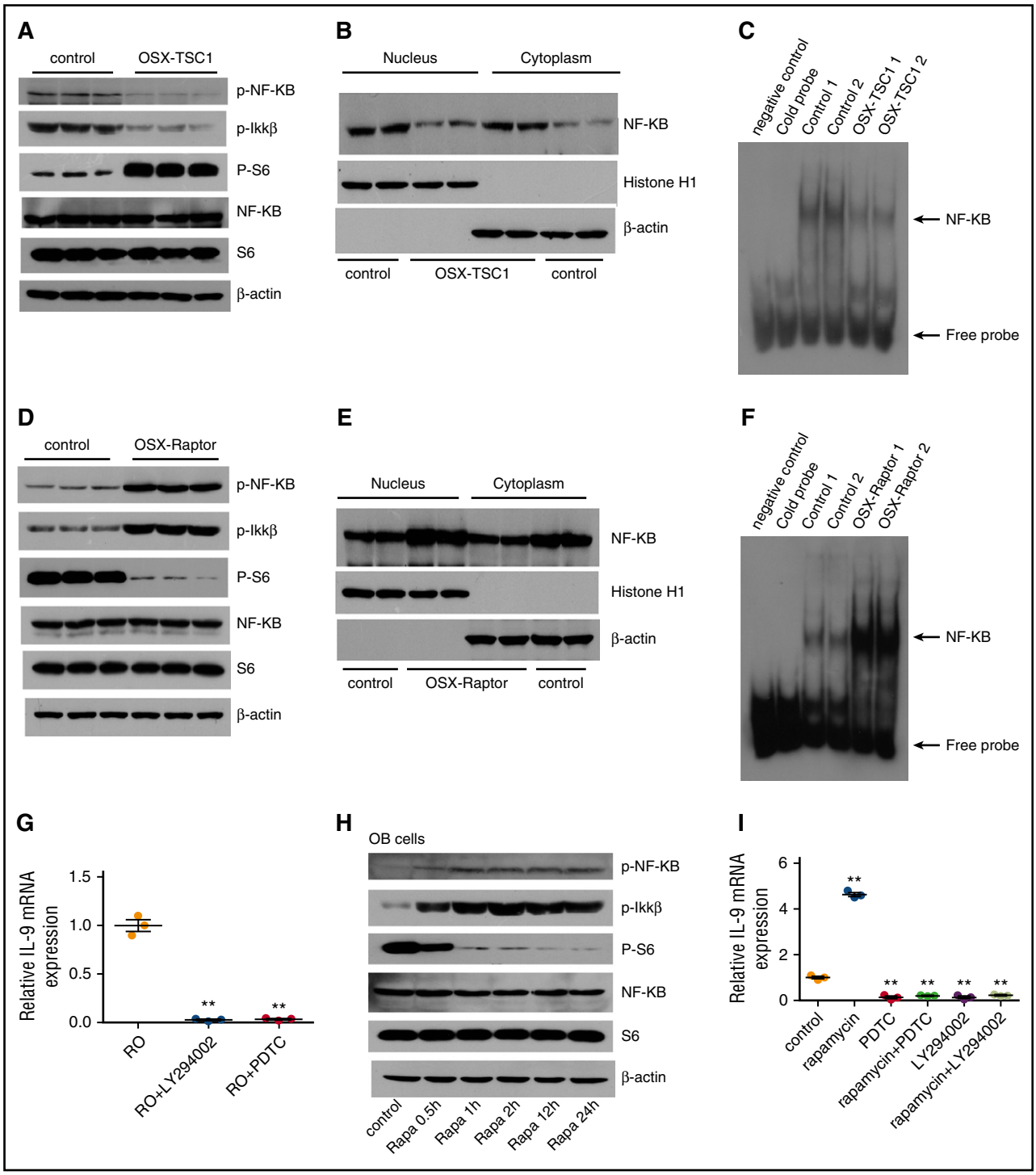


**Figure 5. mTORC1 represses IL-9 transcription through inhibition of NF-κB signaling.** (A) Western blot analysis of *p*-p65NF-κB (S653) and *p*-IKK-β (S180/181) in TSC1-deficient osteoblast. (B) Nuclear and cytosol localization of p65 in TSC1-deficient osteoblasts. Histone H1 and β-actin were used as nuclear and cytosolic protein markers, respectively. (C) EMSA of DNA binding activity of NF-κB to *Il9* gene promoter in the TSC1 deletion or control osteoblasts. (D) Western blot analysis of *p*-p65NF-κB (S653) and *p*-IKK-β (S180/181) in Raptor-deficient osteoblast. (E) Nuclear and cytosolic localization of p65 in Raptor-deficient osteoblasts. Histone H1 and β-actin were used as nuclear and cytosol protein markers, respectively. (F) EMSA of DNA binding activity of NF-κB to *Il9* gene promoter in the Raptor deletion or control osteoblasts. (G) IL-9 mRNA levels in Raptor-deficient osteoblasts (ROs) treated with NF-κB inhibitor (PDTC) or PI3-K/Akt inhibitor (LY294002), as detected by quantitative polymerase chain reaction (n = 3, 1-way ANOVA). (H) Western blot analysis of *p*-p65NF-κB (S653) and *p*-IKK-β (S180/181) in osteoblast (OB) cells treated with 50 nM rapamycin. (I) Quantitative polymerase chain reaction analysis of IL-9 mRNA levels in OBs treated with rapamycin (50 nM) and PDTC (50 μM), or LY294002 (50 μM) (n = 3, 1-way ANOVA). Data are representative of 3 independent experiments and are represented as mean ± SD. $^{**}P < .01$.

activity of neighboring cells in the microenvironment via paracrine mTORC1 signaling, which represents an important but lesser known function of this pathway.

Management of severe thrombocytopenia in patients with malignancies undergoing myelosuppressive chemotherapy remains a significant challenge to practicing hematologists and oncologists.[39]

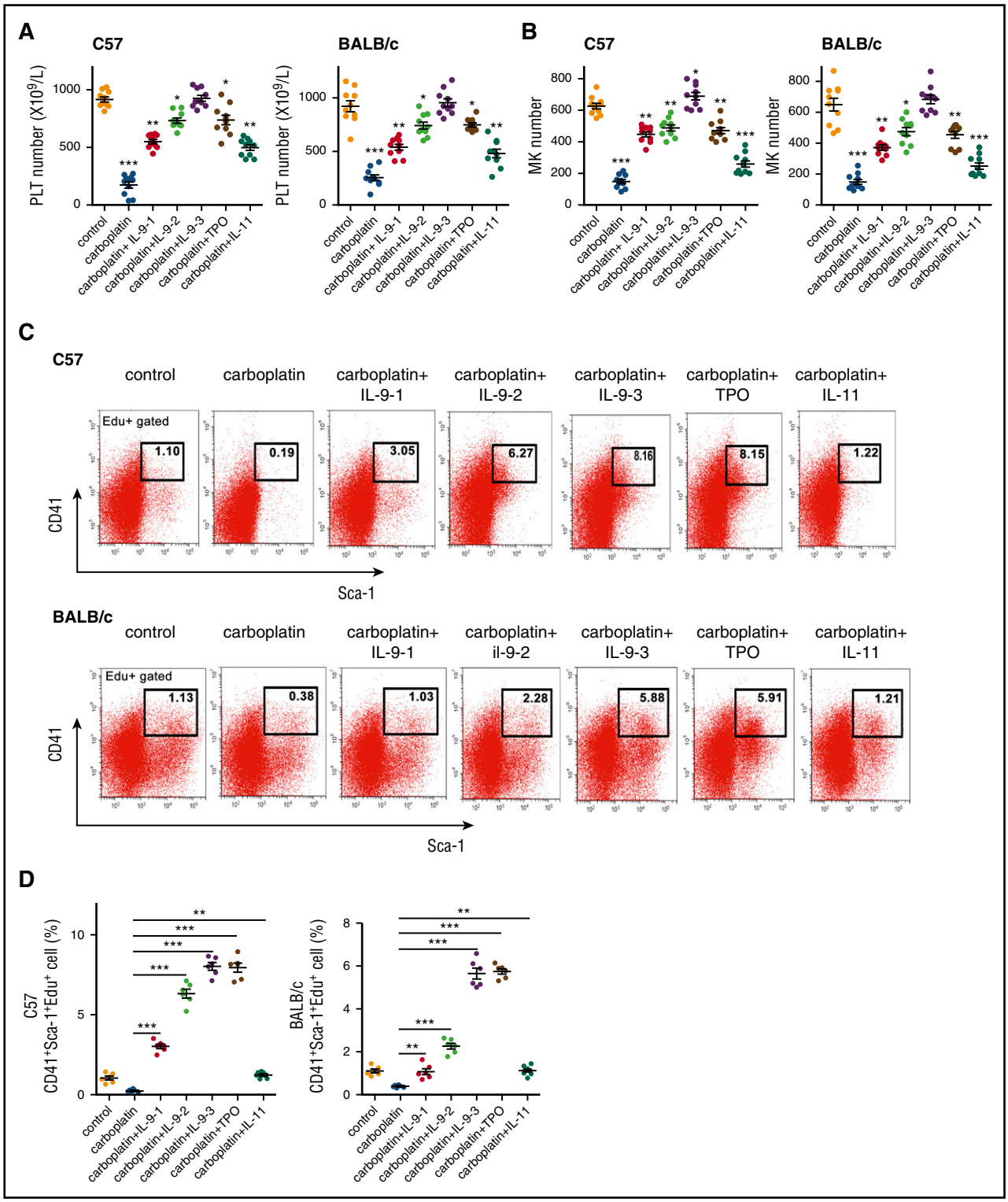


**Figure 6. Low doses of IL-9 prevent chemotherapy-induced thrombocytopenia.** (A) BALB/c and C57BL/6 mice (2 months old) were injected with carboplatin (100 mg/kg) followed by daily injection with IL-9 (1, 2.5, or 7.5 μg/kg per day), TPO (100 μg/kg per day), or IL-11 (100 μg/kg per day) starting on the second day for 8 days. IL-9-1, 2, and 3 represent the dose of 1, 2.5, and 7.5 μg/kg per day, respectively. Mean platelet count was determined (n = 10, 1-way ANOVA). (B) MK counts in mice (n = 10, 1-way ANOVA). (C) FACS analysis of proliferation rate of MK progenitor cells ($CD41^+Sca\text{-}1^+Edu^+$) in BM of treated mice (n = 6, Student unpaired *t* test). (D) Quantification analysis of $CD41^+Sca\text{-}1^+Edu^+$ cells in (C) (n = 6, Student unpaired *t* test). Data are representative of 3 independent experiments and are represented as mean ± SD. $^*P < .05$; $^{**}P < .01$; $^{***}P < .001$.

Multiple cytokines affect platelet formation, and TPO is the physiological regulator of thrombopoiesis.[40] Although promising biologic activity was observed with recombinant TPOs, their clinical application is limited by antibodies that neutralize the recombinant proteins. Several novel TPO receptor (c-Mpl) agonists, including romiplostim and eltrombopag, with lesser potential for immunogenicity

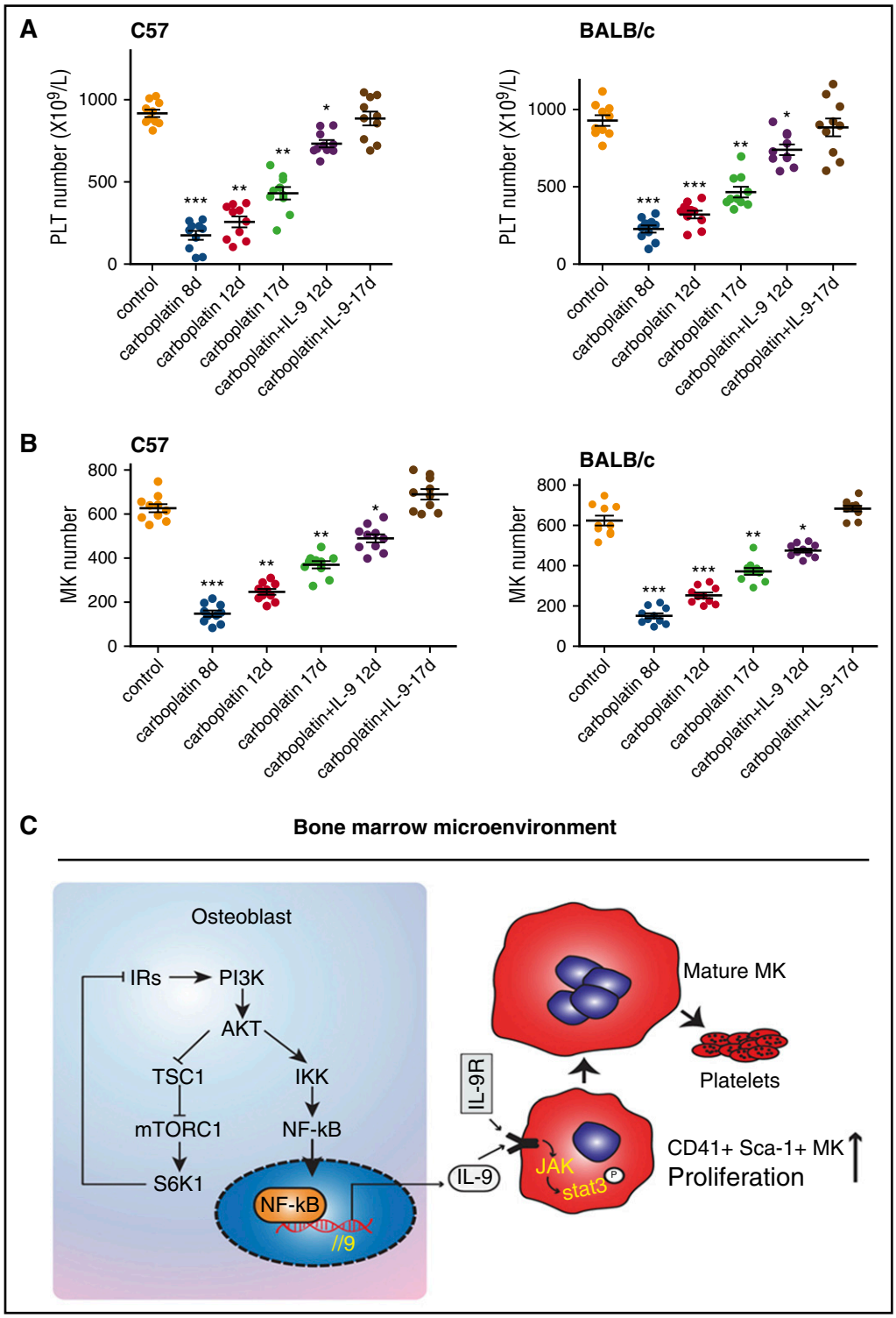


**Figure 7. Low doses of IL-9 accelerate platelet recovery after chemotherapy-induced thrombocytopenia.** (A) C57BL/6 mice (2 months old) were injected with carboplatin (100 mg/kg); 8 days later, mice were treated with IL-9 (IP, 2.5 μg/kg per day) for another 8 days and platelet numbers were counted (n = 10, 1-way ANOVA). (B) MK counts in mice (n = 10, 1-way ANOVA). Data are representative of 3 independent experiments and are represented as mean ± SD. *$P < .05$; **$P < .01$; ***$P < .001$. (C) Schematic model for regulation of megakaryocyte formation by osteoblast through secretion of IL-9. IRs, insulin receptor substrates.

have been developed for immune thrombocytopenia treatment.[41,42] However, they are less effective for patients with severe thrombocytopenia after intensive chemotherapy. Recombinant IL-11 is another agent approved by US Food and Drug Administration for CIT, but its use is restricted due to its narrow therapeutic index.[43] Several lines of evidence from the present in vivo study suggest that IL-9 may be a better option for treatment of CIT than existing agents for the following reasons: (1) IL-9 is more effective than TPO and IL-11 for treatment of severe CIT; (2) IL-9 not only prevents CIT, but accelerates platelet repopulation and shortens the period of severe CIT; and (3) the minimum effective dose

of IL-9 used in this study is very low, which can prevent potential adverse effects such as asthma. Further studies are warranted to evaluate the full therapeutic potential of IL-9 in the treatment of CIT.

## Acknowledgments

The authors thank David J. Kwiatkowski (Brigham and Women's Hospital) for providing $TSC2^{+/+}$ and $TSC2^{-/-}$ MEFs.

This work was supported by grants from National Natural Sciences Foundation of China (31500947, 81625015, U1301222, 81530070, and 31529002), the State Key Development Program for Basic Research of China (2013CB945203 and 2015CB553602), and the Natural Science Foundation of Guangdong Province, China (2016A030313631).

## Authorship

Contribution: X.B., M.X., and Y.J. designed the research and wrote the paper; M.X., Y.W., C.T., Z.W., and J.Y. performed and analyzed the experiments in the transgenic mice; Z.Z., Z.C., M.L., A.L., C.J., B.H., and B.Y. performed cell experiments; P.L., C.D., and D.C. generated mice and genotype identification; G.X. helped to formulate the hypothesis; and X.B. designed and analyzed experiments, supervised the study, and wrote the manuscript, with input from all authors.

Conflict-of-interest disclosure: The authors declare no competing financial interests.

Correspondence: Xiaochun Bai, Department of Cell Biology, School of Basic Medical Sciences, The Third Affiliated Hospital, Southern Medical University, Shatai Nan Rd 1023-1063, Baiyun District, Guangzhou, China 510515; e-mail: baixc15@smu.edu.cn.

## References

1. Angiolillo DJ, Ferreiro JL, Price MJ, Kirtane AJ, Stone GW. Platelet function and genetic testing. *J Am Coll Cardiol*. 2013;62(17 Suppl): S21-S31.
2. Machlus KR Jr, Italiano JE Jr. The incredible journey: from megakaryocyte development to platelet formation. *J Cell Biol*. 2013;201(6): 785-796.
3. Panuganti S, Schlinker AC, Lindholm PF, Papoutsakis ET, Miller WM. Three-stage ex vivo expansion of high-ploidy megakaryocytic cells: toward large-scale platelet production. *Tissue Eng Part A*. 2013;19(7-8):998-1014.
4. Lorenzo J, Horowitz M, Choi Y. Osteoimmunology: interactions of the bone and immune system. *Endocr Rev*. 2008;29(4): 403-440.
5. Lieberman L, Bercovitz RS, Sholapur NS, Heddle NM, Stanworth SJ, Arnold DM. Platelet transfusions for critically ill patients with thrombocytopenia. *Blood*. 2014;123(8): 1146-1151, quiz 1280.
6. Nieswandt B, Stritt S. Megakaryocyte rupture for acute platelet needs. *J Cell Biol*. 2015;209(3): 327-328.
7. Pang L, Weiss MJ, Poncz M. Megakaryocyte biology and related disorders. *J Clin Invest*. 2005; 115(12):3332-3338.
8. Shen Y, Nilsson SK. Bone, microenvironment and hematopoiesis. *Curr Opin Hematol*. 2012;19(4): 250-255.
9. Calvi LM, Adams GB, Weibrecht KW, et al. Osteoblastic cells regulate the haematopoietic stem cell niche. *Nature*. 2003;425(6960): 841-846.
10. Zhang J, Niu C, Ye L, et al. Identification of the haematopoietic stem cell niche and control of the niche size. *Nature*. 2003;425(6960): 836-841.
11. Arai F, Hirao A, Ohmura M, et al. Tie2/ angiopoietin-1 signaling regulates hematopoietic stem cell quiescence in the bone marrow niche. *Cell*. 2004;118(2):149-161.
12. Schepers K, Hsiao EC, Garg T, Scott MJ, Passegué E. Activated Gs signaling in osteoblastic cells alters the hematopoietic stem cell niche in mice. *Blood*. 2012;120(17): 3425-3435.
13. Visnjic D, Kalajzic Z, Rowe DW, Katavic V, Lorenzo J, Aguila HL. Hematopoiesis is severely altered in mice with an induced osteoblast deficiency. *Blood*. 2004;103(9): 3258-3264.
14. Rankin EB, Wu C, Khatri R, et al. The HIF signaling pathway in osteoblasts directly modulates erythropoiesis through the production of EPO. *Cell*. 2012;149(1):63-74.
15. Wu JY, Purton LE, Rodda SJ, et al. Osteoblastic regulation of B lymphopoiesis is mediated by Gsalpha-dependent signaling pathways. *Proc Natl Acad Sci USA*. 2008; 105(44):16976-16981.
16. Lorenzo J, Horowitz M, Choi Y. Osteoimmunology: interactions of the bone and immune system. *Endocr Rev*. 2008; 29(4):403-440.
17. Lemieux JM, Horowitz MC, Kacena MA. Involvement of integrins alpha(3)beta(1) and alpha(5)beta(1) and glycoprotein IIb in megakaryocyte-induced osteoblast proliferation. *J Cell Biochem*. 2010;109(5):927-932.
18. Cheng YH, Hooker RA, Nguyen K, et al. Pyk2 regulates megakaryocyte-induced increases in osteoblast number and bone formation. *J Bone Miner Res*. 2013;28(6):1434-1445.
19. Kacena MA, Shivdasani RA, Wilson K, et al. Megakaryocyte-osteoblast interaction revealed in mice deficient in transcription factors GATA-1 and NF-E2. *J Bone Miner Res*. 2004;19(4): 652-660.
20. Laplante M, Sabatini DM. mTOR signaling in growth control and disease. *Cell*. 2012;149(2): 274-293.
21. Shimobayashi M, Hall MN. Making new contacts: the mTOR network in metabolism and signalling crosstalk. *Nat Rev Mol Cell Biol*. 2014;15(3): 155-162.
22. Tamamyan G, Danielyan S, Lambert MP. Chemotherapy induced thrombocytopenia in pediatric oncology. *Crit Rev Oncol Hematol*. 2016; 99:299-307.
23. Yang YC, Ricciardi S, Ciarletta A, Calvetti J, Kelleher K, Clark SC. Expression cloning of cDNA encoding a novel human hematopoietic growth factor: human homologue of murine T-cell growth factor P40. *Blood*. 1989;74(6): 1880-1884.
24. Raaijmakers MH, Mukherjee S, Guo S, et al. Bone progenitor dysfunction induces myelodysplasia and secondary leukaemia. *Nature*. 2010; 464(7290):852-857.
25. Wright DE, Wagers AJ, Gulati AP, Johnson FL, Weissman IL. Physiological migration of hematopoietic stem and progenitor cells. *Science*. 2001;294(5548):1933-1936.
26. Mundy G, Garrett R, Harris S, et al. Stimulation of bone formation in vitro and in rodents by statins. *Science*. 1999;286(5446):1946-1949.
27. Huang B, Wang Y, Wang W, et al. mTORC1 prevents preosteoblast differentiation through the Notch signaling pathway. *PLoS Genet*. 2015; 11(8):e1005426.
28. Kunicki TJ, Williams SA, Nugent DJ, Yeager M. Mean platelet volume and integrin alleles correlate with levels of integrins $\alpha$(IIb)$\beta$(3) and $\alpha$(2)$\beta$(1) in acute coronary syndrome patients and normal subjects. *Arterioscler Thromb Vasc Biol*. 2012;32(1):147-152.
29. Habart D, Cheli Y, Nugent DJ, Ruggeri ZM, Kunicki TJ. Conditional knockout of integrin $\alpha 2\beta 1$ in murine megakaryocytes leads to reduced mean platelet volume. *PLoS One*. 2013; 8(1):e55094.
30. Rodda SJ, McMahon AP. Distinct roles for Hedgehog and canonical Wnt signaling in specification, differentiation and maintenance of osteoblast progenitors. *Development*. 2006; 133(16):3231-3244.
31. Kaplan MH, Hufford MM, Olson MR. The development and in vivo function of T helper 9 cells. *Nat Rev Immunol*. 2015;15(5): 295-307.
32. Noelle RJ, Nowak EC. Cellular sources and immune functions of interleukin-9. *Nat Rev Immunol*. 2010;10(10):683-687.
33. Goswami R, Kaplan MH. A brief history of IL-9. *J Immunol*. 2011;186(6):3283-3288.
34. Dan HC, Cooper MJ, Cogswell PC, Duncan JA, Ting JP, Baldwin AS. Akt-dependent regulation of NF-kappaB is controlled by mTOR and Raptor in association with IKK. *Genes Dev*. 2008;22(11): 1490-1500.
35. Stassen M, Müller C, Arnold M, et al. IL-9 and IL-13 production by activated mast cells is strongly enhanced in the presence of lipopolysaccharide: NF-kappa B is decisively involved in the expression of IL-9. *J Immunol*. 2001;166(7):4391-4398.
36. Dan HC, Baldwin AS. Differential involvement of IkappaB kinases alpha and beta in cytokine- and insulin-induced mammalian target of rapamycin activation determined by Akt. *J Immunol*. 2008; 180(11):7582-7589.
37. Sun S, Wang W, Latchman Y, Gao D, Aronow B, Reems JA. Expression of plasma membrane receptor genes during megakaryocyte development. *Physiol Genomics*. 2013;45(6): 217-227.

38. Fujiki H, Kimura T, Minamiguchi H, et al. Role of human interleukin-9 as a megakaryocyte potentiator in culture. *Exp Hematol*. 2002;30(12): 1373-1380.

39. Vadhan-Raj S, Kavanagh JJ, Freedman RS, et al. Safety and efficacy of transfusions of autologous cryopreserved platelets derived from recombinant human thrombopoietin to support chemotherapy-associated severe thrombocytopenia: a randomised cross-over study. *Lancet*. 2002; 359(9324):2145-2152.

40. Emerson SG. Thrombopoietin, HSCs, and the osteoblast niche: holding on loosely, but not letting G0. *Cell Stem Cell*. 2007;1(6): 599-600.

41. Imbach P, Crowther M. Thrombopoietin-receptor agonists for primary immune thrombocytopenia. *N Engl J Med*. 2011;365(8):734-741.

42. Kaushansky K, Lok S, Holly RD, et al. Promotion of megakaryocyte progenitor expansion and differentiation by the c-Mpl ligand thrombopoietin. *Nature*. 1994;369(6481): 568-571.

43. Kaye JA. Clinical development of recombinant human interleukin-11 to treat chemotherapy-induced thrombocytopenia. *Curr Opin Hematol*. 1996;3(3):209-215.